TAO, Vol.3, No.4, 533-556, December 1992

# The Composite Structure of Mesolows Accompanying Heavy Rainfall in the Taiwan Mei-Yu Season

GEORGE T.J. CHEN[1] and C.C. WANG[2]

(Received: October 18, 1992; Revised: November 10, 1992)

## ABSTRACT

**Five cases of mesolows accompanying heavy rainfall in the Mei-Yu season of 1985-1987 were studied. Data used consisted of the 3-h surface observations and the 3-h infrared digital data of the cloud top temperature observed by the Geostationary Meteorological Satellite of Japan. A composite technique was used to obtain the structure of each individual mesolow, the structure at the different life stages, and the structure for the different space scales. The composite fields included pressure, temperature, dew-point depression, streamline and isotach, vorticity, divergence, mean cloud top temperature, and frequency of deep convections of different cloud top temperature.**

**It was found that similarities and differences existed among all of the 5 cases. The mesolow which formed and migrated along the Mei-Yu front over the Taiwan Strait had a larger horizontal scale, a longer time duration, and a deeper center pressure as compared to that formed locally to the northwest and southwest of Taiwan. It had heavy rainfall occurrence to the south of the low center where the maximum convergence, the stronger southwesterly flows, and deep convections prevailed, as compared to the locally formed low which had heavy rainfall occurrence over the mesolow area. The blocking effect of the Central Mountain Range (CMR) on the low-level northeasterly cold air appeared to be important in the formation of mesolow to the west of the CMR. The shear vorticity due to the land-sea differential friction was suggested to be important for the formation and maintenance of the mesocyclone over the same area.**

**The composite structure at different life stages showed that the deep convections and thus the heavy rainfall to the south of the low center were closely associated with the formation and intensification of the mesolow through the enhanced southwesterly flows and the boundary layer convergence. The close relationship between the deep convections/heavy rainfall and maximum convergence suggested the important role of the surface boundary layer (frictional) convergence in regulating the behavior of convections. The surface friction also possibly counteracted the vortex stretching process in the evolution of the mesocyclone. Finally, the scale dependent structure was obtained in the composite of the meso-$\alpha$ and meso-$\beta$ lows, similar to that observed in the individual case.**

[1] Department of Atmospheric Sciences, National Taiwan University, Taipei, Taiwan, R.O.C.

[2] Institute of Geoscience, Chinese Culture University, Yangmingshan, Taiwan, R.O.C.

## 1. INTRODUCTION

One of the major findings of an early study on the mesolow in the Taiwan Mei-Yu season by Chen (1978) was a positive correlation existing between rainfall amount and mesolow frequency to the west of the Central Mountain Range (CMR). The maximum cyclogenesis frequency of the mesolow to the west of the CMR was observed over the northwest and southwest of Taiwan in that study. After the presentation of Chen's (1978) paper, the mesolow and the associated rainfall became one of the major interests in the mesoscale study in the Taiwan Mei-Yu season (Chen, 1992).

A close relationship between the heavy rainfall and mesolow was observed over northwestern Taiwan by Chen and Chi (1980). It was suggested that the mesolow over that area probably served as a mechanism for producing heavy rainfall through enhanced southwesterlies. A case study by Chen (1979) showed that the enhancement of convective rainfall was closely related to the mesolow formation and the accompanying wind changes over southwestern Taiwan. This relationship again existed in a recent study by Chen (1990) using 18 cases of heavy rainfall events accompanying mesolows on the west side of the CMR in 1983-1987 Mei-Yu season. In that study the rainfall rate and radar echo intensified substantially during and after mesolow formation. The intensification was suggested to be due to the increase of local convergence which was caused by the increase of pressure gradient and low-level winds to the south of the mesolow.

A case study by Chen (1979) showed that a mesolow on the west coast of Taiwan had a horizontal scale of 200 km and was characterized by strong cyclonic vorticity, horizontal convergence and boundary layer upward motion. Chen and Yu (1990) found the mesolow over southwestern Taiwan was quite shallow (limited to the lowest 1.6 km) with a horizontal scale of 150 km and was responsible for determining the intensity of heavy rainfall in southern Taiwan.

One of the very important issues of the mesolow is the formation mechanism in different geographic areas to the southwest and the northwest of Taiwan. For the mesolow over northwestern Taiwan, a modelling study by Chern and Sun (1989) suggested that the formation is due to subsidence warming and lack of cold advection under the prevailing northeasterly flow to the north of the Mei-Yu front. On the other hand, results of a non-linear semi-geostrophic modelling study by Lin (1989) sugggested that the formation of mesolow over northwestern Taiwan under the prevailing southwesterly barotropic flow was due to diabatic cooling effect which increases the convergence in the mesolow area. For the mesolow over southwestern Taiwan, observational studies suggested that both the convective latent heating (Chen, 1990; Chen and Yu, 1990) and lack of cold air due to the flow blocking by the CMR (Chen *et al.*, 1989; Chen and Hui, 1990; Chen and Liang, 1992) are possible formation mechanisms. Numerical study by Lin (1989) using a non-linear semi-geostrophic model, on the other hand, suggested that a possible mechanism might be diabatic cooling effect which increases convergence over the mesolow area under the prevailing northwesterly baroclinic flow.

From the previous studies, a close relationship was found between the heavy rainfall event and the existence of mesolow to the west of the CMR. However, the questions such as detailed structure and dynamic processes of the mesolow as well as the specific dynamic link between the convection and the mesolow remain unanswered and need for further research. The purpose of this paper is to study these questions by using the composite techinque for five cases of mesolow which accompany heavy rainfall in the Taiwan Mei-Yu season of 1985-1987.

Table 1. Case period, duration, and formation region of 5 mesolows and the relative position of heavy rainfall to mesolow.

| Case no. | Case period | Duration (h) | Formation region | Heavy rainfall occurrence |
|---|---|---|---|---|
| 1 | 1200 UTC 28 - 0000 UTC 29 May 1985 | 12 | northwest of Taiwan | over the mesolow |
| 2 | 1200 UTC 7 - 1200 UTC 8 June 1985 | 24 | west of 118° E | south and southeast of the mesolow |
| 3 | 2100 UTC 13 - 0900 UTC 14 May 1986 | 12 | southwest of Taiwan | over the mesolow |
| 4 | 0600 UTC 6 - 0300 UTC 7 June 1986 | 21 | southwest of Taiwan | over the mesolow |
| 5 | 1500 UTC 24 - 0600 UTC 25 June 1987 | 15 | west of 118° E | south of the mesolow |

## 2. DATA AND ANALYSIS PROCEDURE

Among the 15 cases of mesolow accompanying heavy rainfall, analyzed by Chen and Yu (1988) in the Taiwan Mei-Yu season of 1985-1987, 5 cases were selected in this study mainly because these lows had better data coverage and better organized cyclonic circulations. Data used in this study consisted of the surface weather maps analyzed by the Japan Meteorological Agency (JMA) and the Central Weather Bureau (CWB); the 3-h observations at the surface stations of the CWB, the Chinese Air Force (CAF), and the Civil Aeronautics Administration (CAA); the 3-h ship reports over the adjacent ocean; and the 3-h infrared digital data of the cloud top temperature observed by the Geostationary Meteorological Satellite (GMS) of the JMA. Reanalyses of the surface pressure and streamline were first carried out to better locate the mesolow in the area of 21-26°N and 118-124°E. A mesolow here was defined when (1) a low pressure with closed isobar can be identified when analyzed at 1 hPa intervals or (2) a low pressure can not be analyzed with closed isobar at 1 hPa intervals, but a cyclonic circulation can be identified near the relatively low pressure area. Based on the damage consideration, the criterion of heavy rainfall, greater than 60 mm within 6 h, used by Chen and Yu (1988) was adopted in this study.

Table 2. Classification of life stages of each mesolow case based on the mean ($\bar{V}$) and maximum ($V_{max}$) wind speeds over the cyclonic circulation area of a mesolow and the mean relative vorticity ($\bar{\zeta}$) near vortex center by averaging 4 grids. Unit in knot (0.5 $ms^{-1}$) for wind speed and $10^{-4}$ $s^{-1}$ for relative vorticity. First 2 digits for time indicate date; last 2 digits, for UTC. An * indicates vortex center can not be identified.

| Case no. \ Life stage | | Intensifying | | | Mature | | | | Decaying | | |
|---|---|---|---|---|---|---|---|---|---|---|---|
| 1 | Time | | | | 2812 | 2815 | | | 2818 | 2821 | 2900 |
| | $\bar{V}$ | | | | 6.2 | 5.4 | | | 4.9 | 6.0 | |
| | $V_{max}$ | | | | 18.0 | 14.0 | | | 13.0 | 13.0 | * |
| | $\bar{\zeta}$ | | | | 3.0 | 2.5 | | | 1.4 | 2.4 | |
| 2 | Time | 0712 | 0715 | 0718 | 0721 | 0800 | 0803 | 0806 | 0809 | 0812 | |
| | $\bar{V}$ | 6.2 | 3.8 | 5.9 | 8.3 | 7.7 | 8.5 | 8.6 | 6.7 | 3.4 | |
| | $V_{max}$ | 12.0 | 7.0 | 9.0 | 12.0 | 10.0 | 16.0 | 13.0 | 10.0 | 6.0 | |
| | $\bar{\zeta}$ | 0.8 | 1.0 | 1.4 | 2.4 | 2.4 | 2.7 | 2.6 | 2.5 | 1.7 | |
| 3 | Time | 1321 | | | 1400 | 1403 | | | 1406 | 1409 | |
| | $\bar{V}$ | 5.9 | | | 7.0 | 9.1 | | | 5.9 | | |
| | $V_{max}$ | 11.0 | | | 12.0 | 15.0 | | | 12.0 | * | |
| | $\bar{\zeta}$ | 2.3 | | | 2.3 | 2.5 | | | 2.7 | | |
| 4 | Time | 0606 | 0609 | 0612 | 0615 | 0618 | | | 0621 | 0700 | 0703 |
| | $\bar{V}$ | 5.7 | 5.4 | 5.9 | 6.7 | 5.3 | | | 4.4 | 6.3 | |
| | $V_{max}$ | 10.0 | 10.0 | 11.0 | 11.0 | 10.0 | | | 8.0 | 10.0 | * |
| | $\bar{\zeta}$ | 1.4 | 2.2 | 1.8 | 1.7 | 2.2 | | | 1.6 | 2.3 | |
| 5 | Time | 2415 | | | 2418 | 2421 | | | 2500 | 2503 | 2506 |
| | $\bar{V}$ | 9.1 | | | 11.5 | 9.0 | | | 8.2 | 5.8 | |
| | $V_{max}$ | 16.0 | | | 22.0 | 18.0 | | | 15.0 | 8.0 | * |
| | $\bar{\zeta}$ | 2.9 | | | 3.8 | 4.7 | | | 3.2 | 1.7 | |
| Time periods for compositing | | 8 | | | 12 | | | | 13 | | |

The case period and the formation region of 5 mesolows selected and the relative position of heavy rainfall occurrence with respect to the mesolow are summarized in Table 1. Case 2 and case 5 originated to the west of 118°E then moved into Taiwan area to affect the central and northern Taiwan area. Case 1 formed to the northwest of Taiwan; cases 3 and 4, to the southwest. The heavy rainfall occurred to the south of mesolow for cases 2 and 5, and over the mesolow area for cases 1, 3, and 4. The mean duration for these 5 cases was 17 h, somewhat longer than 12-15 h obtained by Chen (1978) and Chen and Yu (1988).

All the fields, such as wind, pressure, temperature and humidity were subjectively analyzed and digitized at 0.25° longitude by 0.25° latitude grids within a 3° longitude by 3° latitude region centerd at the cyclonic center of the mesolow. The GMS infrared cloud top temperatures were obtained at 0.2° longitude-latitude grids. To define the different life stages of a mesolow, three parameters were obtained. These are the mean and maximum wind speeds over the cyclonic circulation area of a mesolow and the mean relative vorticity near vortex center, as obtained by averaging 4 grids over the center. Table 2 shows the variations of these parameters for each case and the classification of life stages. The different

Table 3. Horizontal scale of the cyclonic circulation area of each mesolow case during its life period. A * indicates no circulation can be identified. First 2 digits in time indicate date; last 2 digits, UTC.

| Case no. | | Time and scale (km) | | | | | | | | |
|---|---|---|---|---|---|---|---|---|---|---|
| 1 | Time | 2812 | 2815 | 2818 | 2821 | 2900 | | | | |
| | Scale | 160 | 130 | 120 | 100 | * | | | | |
| 2 | Time | 0712 | 0715 | 0718 | 0721 | 0800 | 0803 | 0806 | 0809 | 0812 |
| | Scale | 400 | 350 | 370 | 400 | 400 | 300 | 300 | 200 | 200 |
| 3 | Time | 1321 | 1400 | 1403 | 1406 | 1409 | | | | |
| | Scale | 120 | 100 | 150 | 160 | * | | | | |
| 4 | Time | 0606 | 0609 | 0612 | 0615 | 0618 | 0621 | 0700 | 0703 | |
| | Scale | 100 | 100 | 150 | 150 | 190 | 180 | 180 | * | |
| 5 | Time | 2415 | 2418 | 2421 | 2500 | 2503 | 2506 | | | |
| | Scale | 250 | 200 | 150 | 150 | 100 | * | | | |
| Remarks | | Number of time periods: 11 for meso-$\alpha$ scale ($\geq$ 200 km), 22 for meso-$\beta$ scale (< 200 km). | | | | | | | | |

life stages were defined by the following criteria: (1) The time period covering the time of a substantial increase to the time of a substantial decrease of three parameters was classified as the mature stage; the earlier time period as the intensifying stage and the later time period as the decaying stage. (2) When the variation of one of the three parameters was not obvious or differed from the other two, the life stages were then defined mainly by the other two parameters. (3) When the time period could be classified into either one of the two stages, it was assigned to the stage which had fewer time periods.

Although the surface data coverage was reasonably good for the mesoscale analyses over Taiwan area, it was relatively sparse over the adjacent ocean even considering all the available ship reports. To alleviate this problem, the composite technique was employed to cover the entire life period for each individual mesolow case. Hopefully, the similarities and the differences among various mesolows can be identified. To better understand the structure and dynamic processes during the life time of a mesolow, composite technique was used for each stage as classified in Table 2. The horizontal scale, as defined by the cyclonic circulation area of mesolow, can either be varied from time to time for one case or differed among cases as indicated in Table 3. Thus, the composite technique was also applied to the meso-$\alpha$ ($\geq$ 200 km) and meso-$\beta$ ( < 200 km) scale lows to reveal the possible differences between these two scales. Once the composite streamlines and isotachs were obtained, the horizontal divergence and relative vorticity fields were then computed using a centered finite difference scheme. All the composite fields were presented and discussed within a 2° longitude by 2° latitude region centered at the cyclonic mesolow center, although the subjectively digitized data covered a much larger region.

## 3. COMPOSITE STRUCTURE OF INDIVIDUAL CASE

The composite fields, such as pressure, temperature, temperature dew-point depression, streamline, isotach, vorticity, and divergence, were obtained based on the 3-h surface observations. The surface temperature reflected the elevation effect besides the mesolow structure and the distribution of the temperature dew-point depression was rather similar among cases and relatively uniform over the mesolow area. Thus, the composite temperature and humidity fields will be discussed, but they will not be presented. The composite cloud fields derived from the GMS infrared cloud top temperatures included the mean cloud top temperature, the frequencies of deep convections with cloud top temperatures < -32°C, < -52°C, and < -61°C. Although all of the cloud parameters will be discussed, only the mean cloud top temperatures will be presented here.

### 3.1 Case 1: 28-29 May 1985

Composite fields of case 1 are presented in Figure 2. In this case, the mesolow formed over northwestern Taiwan (Figure 1) and the heavy rainfall occurred over the mesolow area (Table 1). The horizontal scale of the pressure field was rather small with a relatively small perturbation amplitude (the difference of center pressure from the environment mean), being about 1.5 hPa. However, the surface front can be identified by the pressure kink, in agreement with the original surface analyses. The high pressure ridge to the south of the low center was a reflection of the pressure reduction with a temperature trough (not shown) over the same area. Relatively warm and moist air prevailed over the center and its immediate vicinities (not shown).

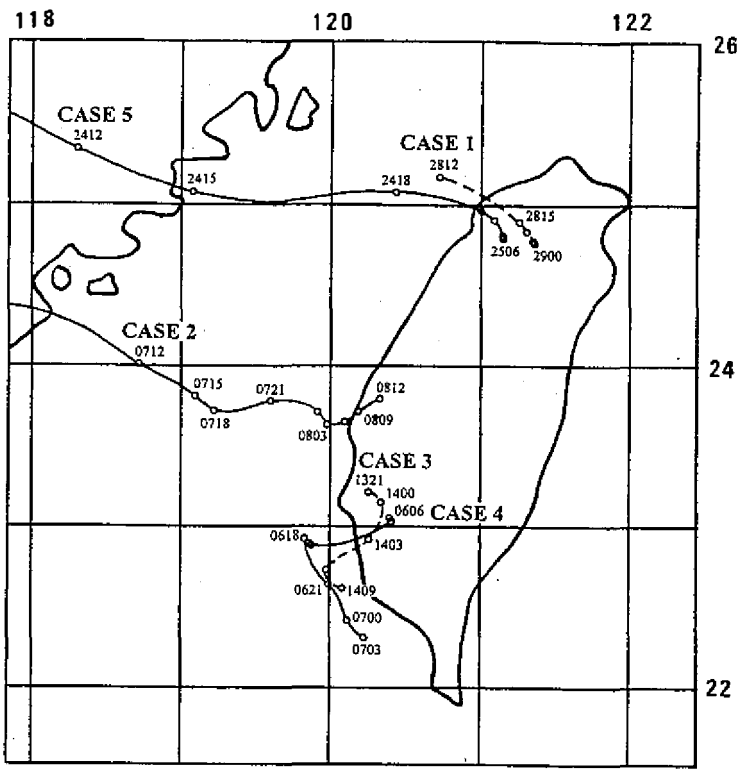


*Fig. 1.* Tracks of 5 mesolows selected. First two digits indicate date; last two, UTC.

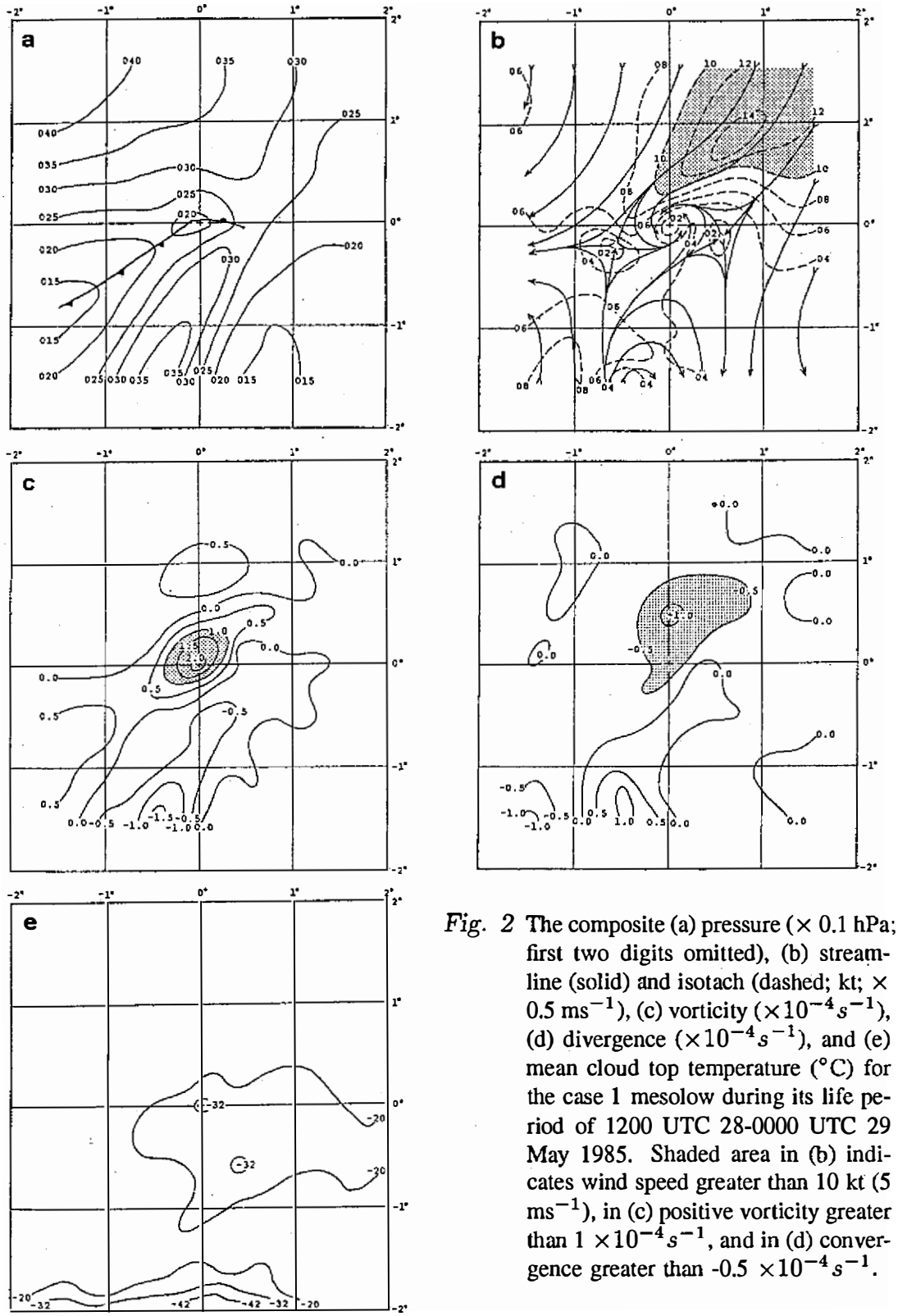


*Fig. 2* The composite (a) pressure (× 0.1 hPa; first two digits omitted), (b) streamline (solid) and isotach (dashed; kt; × 0.5 $ms^{-1}$), (c) vorticity ($\times 10^{-4} s^{-1}$), (d) divergence ($\times 10^{-4} s^{-1}$), and (e) mean cloud top temperature (°C) for the case 1 mesolow during its life period of 1200 UTC 28-0000 UTC 29 May 1985. Shaded area in (b) indicates wind speed greater than 10 kt (5 $ms^{-1}$), in (c) positive vorticity greater than 1 $\times 10^{-4} s^{-1}$, and in (d) convergence greater than -0.5 $\times 10^{-4} s^{-1}$.

Cyclonic vortex, centered at the low center, was quite clear under the large-scale prevailing northeasterlies. The horizontal scale as delineated by the composite pressure and streamline for this case was on the order of 100 km. The maximum wind (14 kt) and the maximum gradient in the prevailing northeasterlies to the northeast of the center were mainly due to the land-sea differential friction as the low center located to the northwest of Taiwan. Cyclonic vorticity was a maximum near center ($2 \times 10^{-4}$ $s^{-1}$) with a NE-SW oriented axis approximately over the pressure trough/front area. Horizontal convergence prevailed over the mesolow area with a maximum value of $-1 \times 10^{-4}$ $s^{-1}$ to the north of the center. Over the low center, the mean cloud top temperature was a minimum (-32°C) and the frequency of deep convections was a maximum (not shown), consistent with the heavy rainfall occurrence within the mesolow area. The deepest convection (< -70°C) only occurred over the low center, indicating the important role of the mesolow circulation in producing the heavy rainfall over the mesolow region in this case.

### 3.2 Case 2: 7-8 June 1985

Composite fields of case 2 are presented in Figure 3. In this case, the mesolow originated to the west of 118°E then moved eastward into central western Taiwan (Figure 1) and the heavy rainfall occurred to the south and southeast of the low center (Table 1). The horizontal scale of the pressure field was rather large with a relatively larger perturbation amplitude, being about 2.5 hPa. The NE-SW oriented front can be located by the pressure trough, in agreement with the frontal wave structure in the original surface analyses. The warm tongue extended from the southwest into the low center and the moist air prevailed over the south and southeast area (not shown).

Cyclonic vortex, centered at the low center, over the mesolow area had a relatively large horizontal scale of 350 km. Wind speeds were weaker to the northeast of the low center but stronger to the northwest as compared to the case 1. Cyclonic vorticity was a maximum near center ($2 \times 10^{-4}$ $s^{-1}$) with a NE-SW oriented axis approximately over the surface front. Horizontal convergence prevailed over the mesolow area with a maximum value of $-1 \times 10^{-4}$ $s^{-1}$ to the south and southwest of the center. An area of the minimum mean cloud top temperature was located to the south and southeast of the center. Over the same area, maximum frequency of the deep convections was also observed. Therefore, the heavy rainfall occurred to the south and southeast of the mesolow center where the moist air and the deep convections were also observed.

### 3.3 Case 3: 13-14 May 1986

Composite fields of case 3 are presented in Figure 4. In this case, the mesolow formed to the southwest of Taiwan (Figure 1) and the heavy rainfall occurred over the mesolow area (Table 1). The pressure field was rather weak with a perturbation amplitude of about 1.5 hPa. The high pressure ridge to the east and northeast of the low center was again a reflection of the pressure reduction problem over the high terrain. This is consistent with a temperature trough over the same area. Warm and moist air prevailed over the center and its vicinities.

Cyclonic vortex over the mesolow area, although small in scale, was quite evident. The horizontal scale as delineated by the composite pressure and steamline was on the order of 150 km. The weaker winds over the eastern region and the stronger winds over the western region reflected the land-sea differential friction and the blocking effect of the CMR under the prevailing low-level northeasterlies. Both the cyclonic vorticity and convergence reached a maximum near the mesolow center, in agreement with the heavy rainfall occurrence. The eastern mountainous region had minimum mean cloud top temperatures and maximum

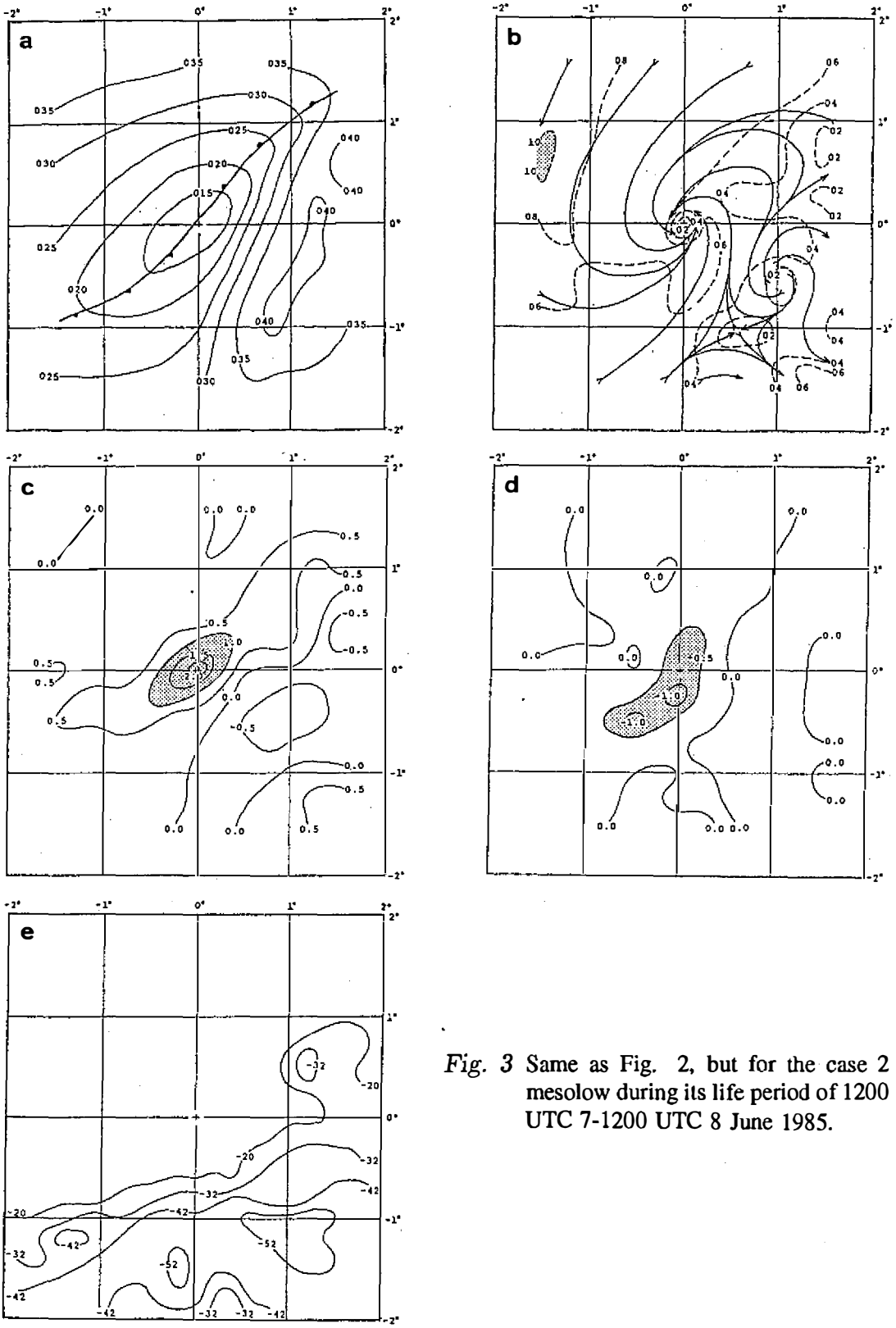


*Fig. 3* Same as Fig. 2, but for the case 2 mesolow during its life period of 1200 UTC 7-1200 UTC 8 June 1985.

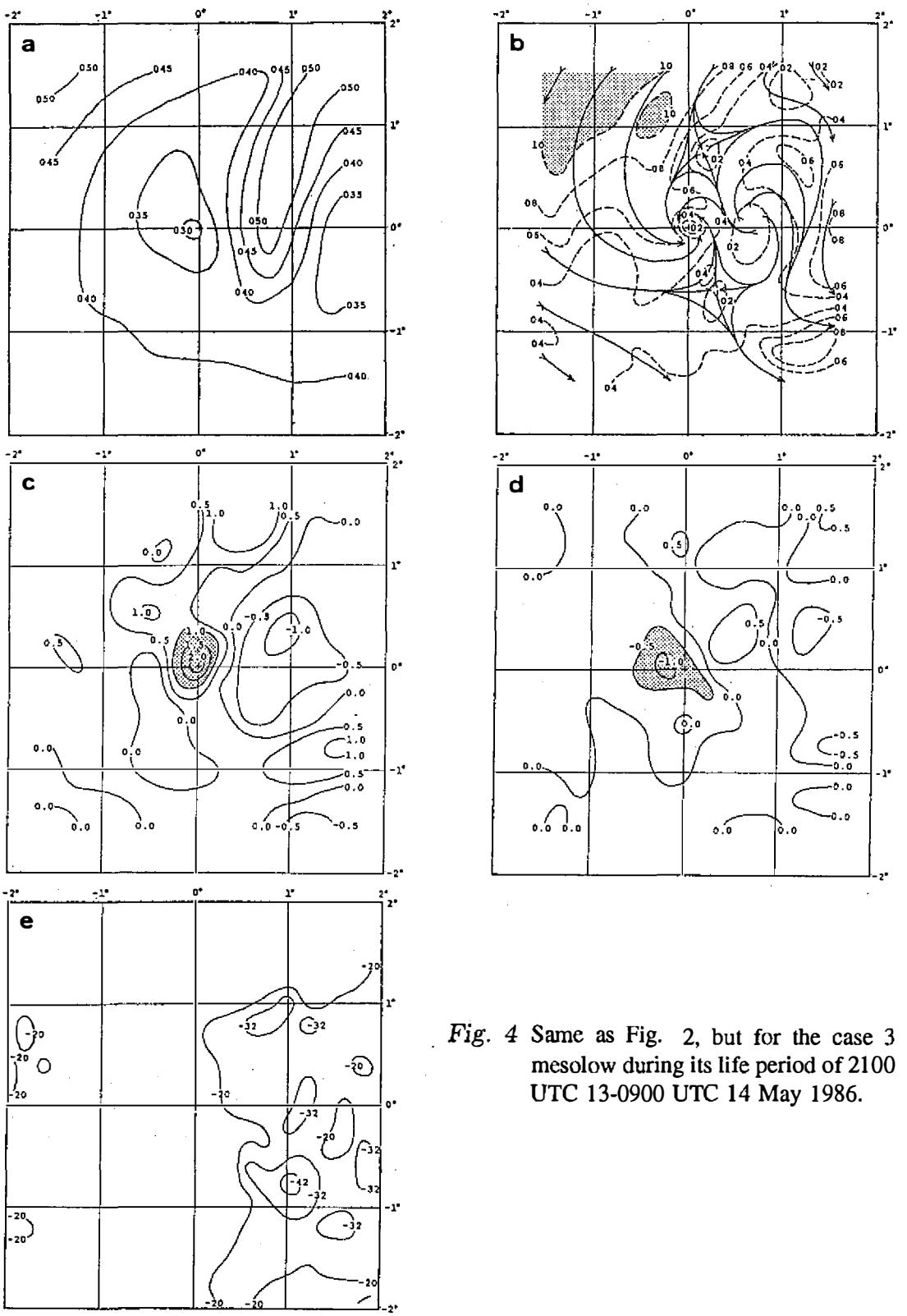


*Fig. 4* Same as Fig. 2, but for the case 3 mesolow during its life period of 2100 UTC 13-0900 UTC 14 May 1986.

frequency of deep convections (not shown), indicating possible heavy rainfall occurrence over the same area. There was a tendency for stronger deep convections (i.e. lower cloud top temperature) to occur near the center. Thus, the heavy rainfall not only occurred over the mesolow area but also possibly prevailed over the CMR where the surface observations were not available.

### 3.4 Case 4: 6-7 June 1986

Composite fields of case 4 are presented in Figure 5. Similar to case 3, the mesolow formed to the southwest of Taiwan (Figure 1) and the heavy rainfall occurred over the mesolow area in this case (Table 1). Although the composite structure was similar to that of the case 3, this mesolow was quite weak with a perturbation pressure of 1 hPa and the horizontal scale was about 180 km. The maximum cyclonic vorticity ($1.5 \times 10^{-4}$ $s^{-1}$) and maximum convergence ($-0.5 \times 10^{-4}$ $s^{-1}$) over the center were also somewhat weaker than those in the case 3. The minimum mean cloud top temperature and the maximum frequency of deep convections were, again similar to those in the case 3, observed to the east of the center. However, the stronger deep convections had a tendency to occur near the center.

### 3.5 Case 5: 24-25 June 1987

Composite fields of case 5 are presented in Figure 6. Heavy rainfall occurred to the south of the mesolow center. Although this mesolow originated to the west of 118°E, it affected northwestern Taiwan for most of its life span. Thus, the composite structure was quite similar to that of the case 1 as would be expected. The horizontal scale of 200 km and perturbation pressure of 2 hPa were somewhat larger than those in case 1 (100 km; 1.5 hPa). Both the cyclonic vorticity and convergence had a maximum over the center with an axis oriented in a NE-SW direction extending towards southwest. The minimum mean cloud top temperature and the maximum frequency of deep convections occurred to the south of low in agreement with the heavy rainfall observation.

### 3.6 Differences and similarities

Since each of the 5 mesolows discussed above was associated with a cyclonic vortex, it can be called a mesocyclone. From the composite structure, it is clear that differences and similarities existed among all of the 5 cases. The horizontal scale of the composite cyclonic vortex for each mesolow was comparable to the mean size of vortex presented in Table 3. The migrating lows along the Mei-Yu front, such as case 2 and case 5, had a larger horizontal size as compared to those formed locally to the northwest (case 1) and southwest (case 3, 4) of Taiwan. They had deeper center pressure (1001.5~1002 hPa) and larger perturbation amplitude (2~2.5 hPa), comparing to the center pressure of 1002~1006 hPa and perturbation amplitude of 1~1.5 hPa for the locally formed lows. Also, the mesolow with a larger horizontal size seemed to have longer life span. Theoretically, a geostrophic relationship between the pressure and the wind fields could not be expected for these mesoscale lows. This was cleary illustrated in the composite pressure and wind fields. Although the cyclonic circulation over the mesoscale low/trough area as well as anticyclonic circulation over the mesoscale high/ridge area was quite evident, the importance of ageostrophic winds was clearly indicated not only over the land/mountainous area but also over the ocean.

The circulation structure of case 1 was quite similar to that of case 5 with minor differences, reflecting the general environment in compositing wind field over northwestern Taiwan for both cases. This is also true in cases 3 and 4 for both of them were located over

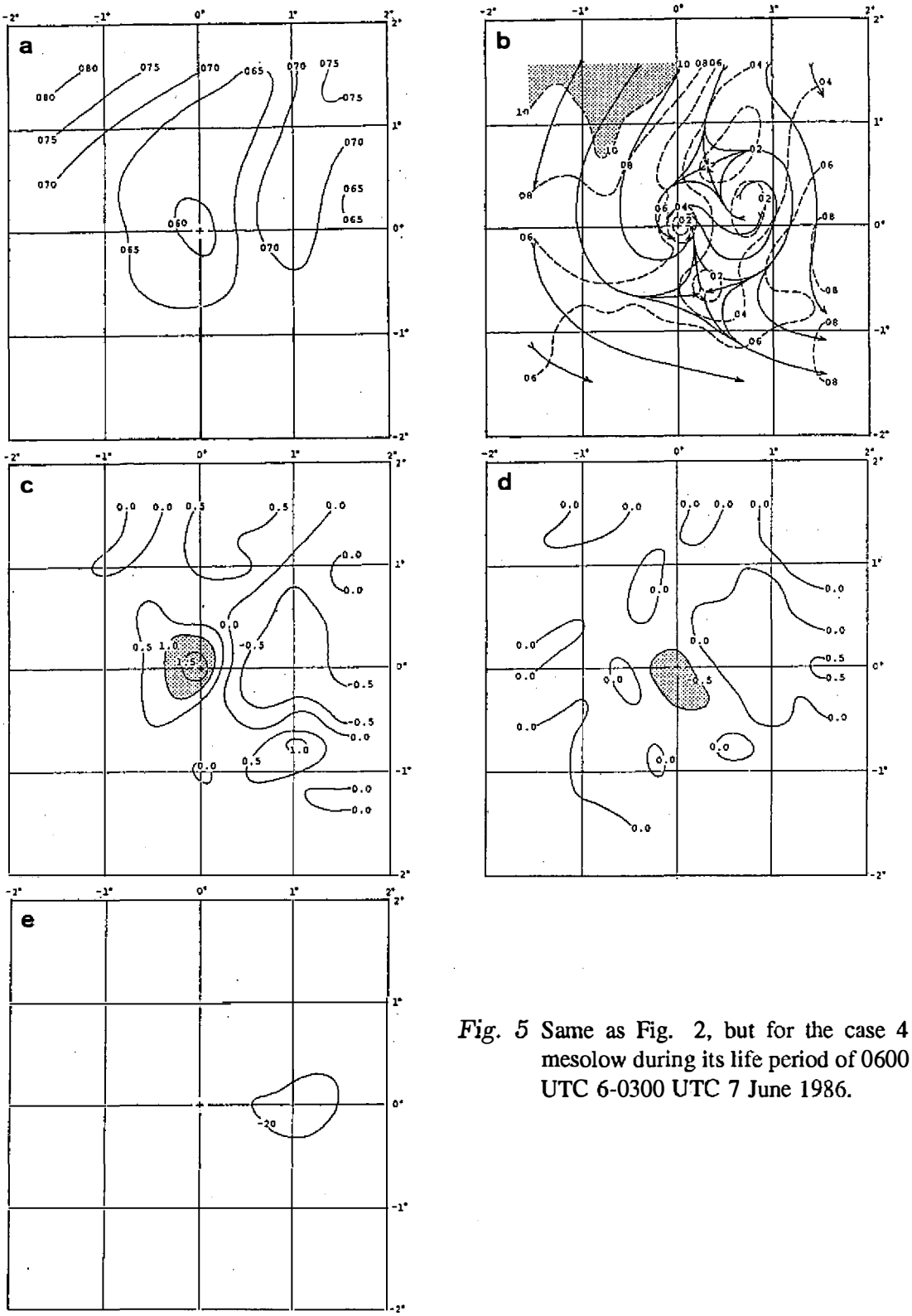


*Fig. 5* Same as Fig. 2, but for the case 4 mesolow during its life period of 0600 UTC 6-0300 UTC 7 June 1986.

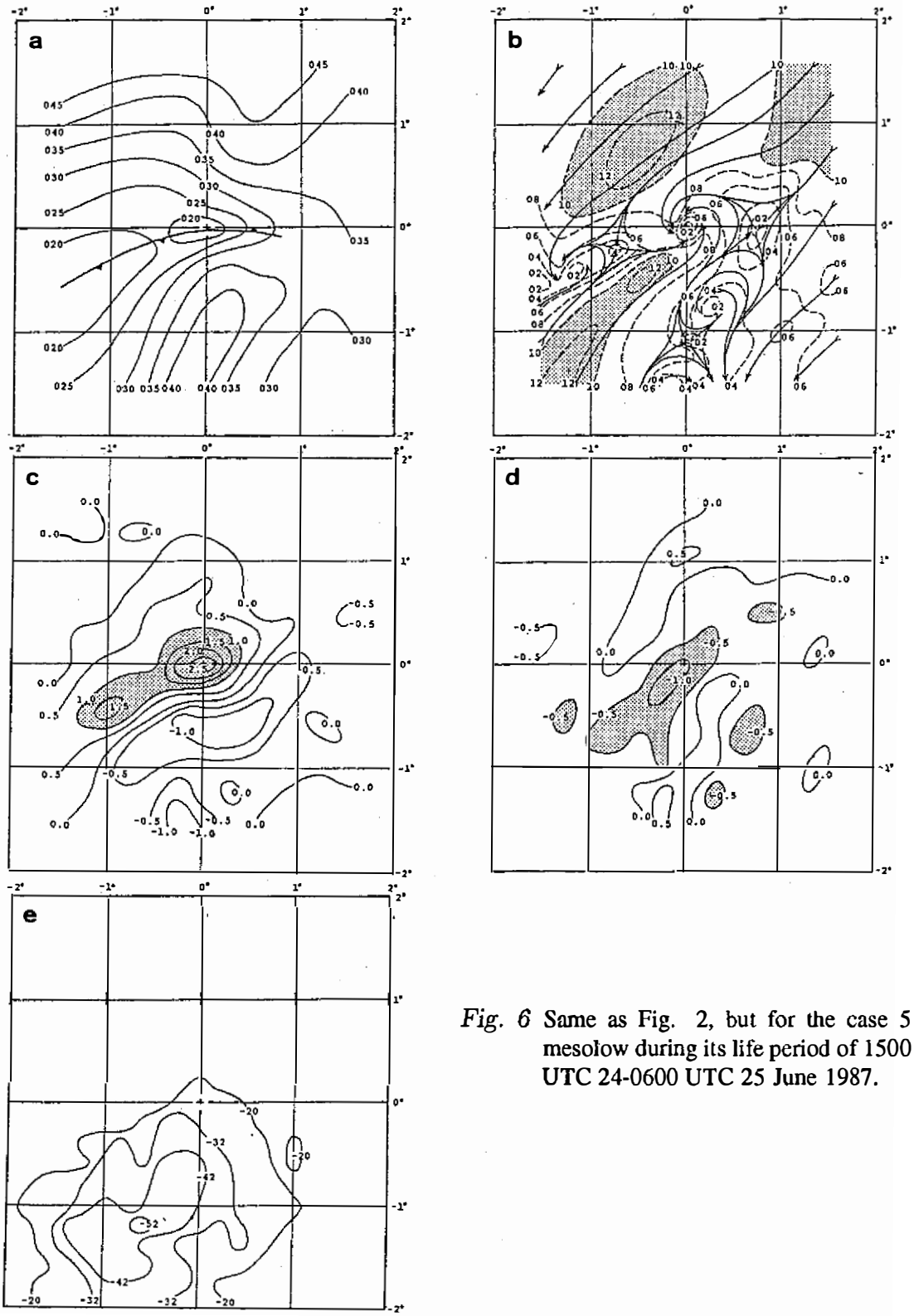


*Fig. 6* Same as Fig. 2, but for the case 5 mesolow during its life period of 1500 UTC 24-0600 UTC 25 June 1987.

southwestern Taiwan. Mesolows in cases 1 and 5 were embedded in the prevailing northeasterly flows with maximum wind (> 12 kt) located very close to the vortex center. Mesolows in cases 3 and 4, on the other hand, were embedded in the prevailing north-northeasterly flows with somewhat weaker maximum wind (> 10 kt) located to the northwest farther away from the low center. The different direction in prevailing wind as well as the weaker winds for the mesolows over southwestern Taiwan indicated the important blocking and deflecting effects of the CMR. The blocking of the low level northeasterly cold air in the Mei-Yu season by the CMR was suggested as one of the possible mechanisms for the mesolow formation over northwestern (Chern and Sun, 1989) and southwestern Taiwan (Chen *et al.*, 1989; Chen and Hui, 1990; Chen and Liang, 1992). Another interesting feature of the composite circulation in cases 1, 3 ,4 and 5 was that the wind speed was much stronger in the prevailing flow over the ocean. Thus, the shear vorticity, mainly attributed to the land-sea differential friction, perhaps was an important vorticity source for the formation and maintenance of the mesocyclone over northwestern and southwestern Taiwan.

Cyclonic vorticity was a maximum over the mesolow center for all cases. An axis of maximum cyclonic vorticity oriented in a NE- SW direction, approximately along the Mei-Yu front, was evident for cases 1, 2, and 5. Horizontal convergence was found to have quite similar distribution and same order of magnitude to those of the cyclonic vorticity. Taking a typical value of convergence near center ($-1 \times 10^{-4}$ $s^{-1}$), it takes the mesolow to double its intensity (in terms of cyclonic vorticity) within 2 h solely due to the vortex stretching process. The fact that this kind of rapid intensity change did not occur (Table 2) suggests the importance of the surface frictional dissipation process in the mesolow dynamics. For cases 2 and 5, which had heavy rainfall observed to the south of the mesolow, convergence maximum prevailed over the center and the southwest. For cases 1, 3 and 4, which had heavy rainfall occurring over the mesolow, convergence maximum was observed mainly over the center area. This seems to suggest that the surface boundary layer convergence plays an important role in regulating the behavior of convections, and thus the heavy rainfall. The distribution of mean cloud top temperature and frequency of deep convections, correlating with the heavy rainfall occurrence, appeared to support this argument.

## 4. COMPOSITE STRUCTURE AT DIFFERENT STAGES

As discussed in the previous section, the gross feature in the composite structure among all of the 5 cases exhibited similarities and differences. To reveal the general characteristics of the mesolow at its different life stages, composite structure was obtained based on the stage classification presented in Table 2. The distribution of the composite dataset appeared to be reasonably uniform at different stages. Although the composite structure for all the parameters was obtained, only that of the pressure, temperature, streamline/isotach, vorticity, divergence, and mean cloud top temperature will be presented here. The composite structure at different stages is illustrated in Figures 7, 8, and 9. Similar tendencies of the mean wind speed, $\bar{V}$, and maximum wind speed, Vmax, over the cyclonic circulation area and the mean relative vorticity, $\bar{\zeta}$, near the vortex center existed during the life cycle of the individual case presented in Table 2 and of the composite presented in Figures 7-9. It is, therefore, reasonable to expect that the structure and evolution processes of the mesolow were well represented by this composite. The composite pressure showed an increase in gradient to the south of the low center and in perturbation amplitude from the intensifying stage to the mature stage and a decrease afterwards. The pressure gradient change was in agreement with the wind speed increase over the same area. The horizontal scale, as delineated by the cyclonic circulation

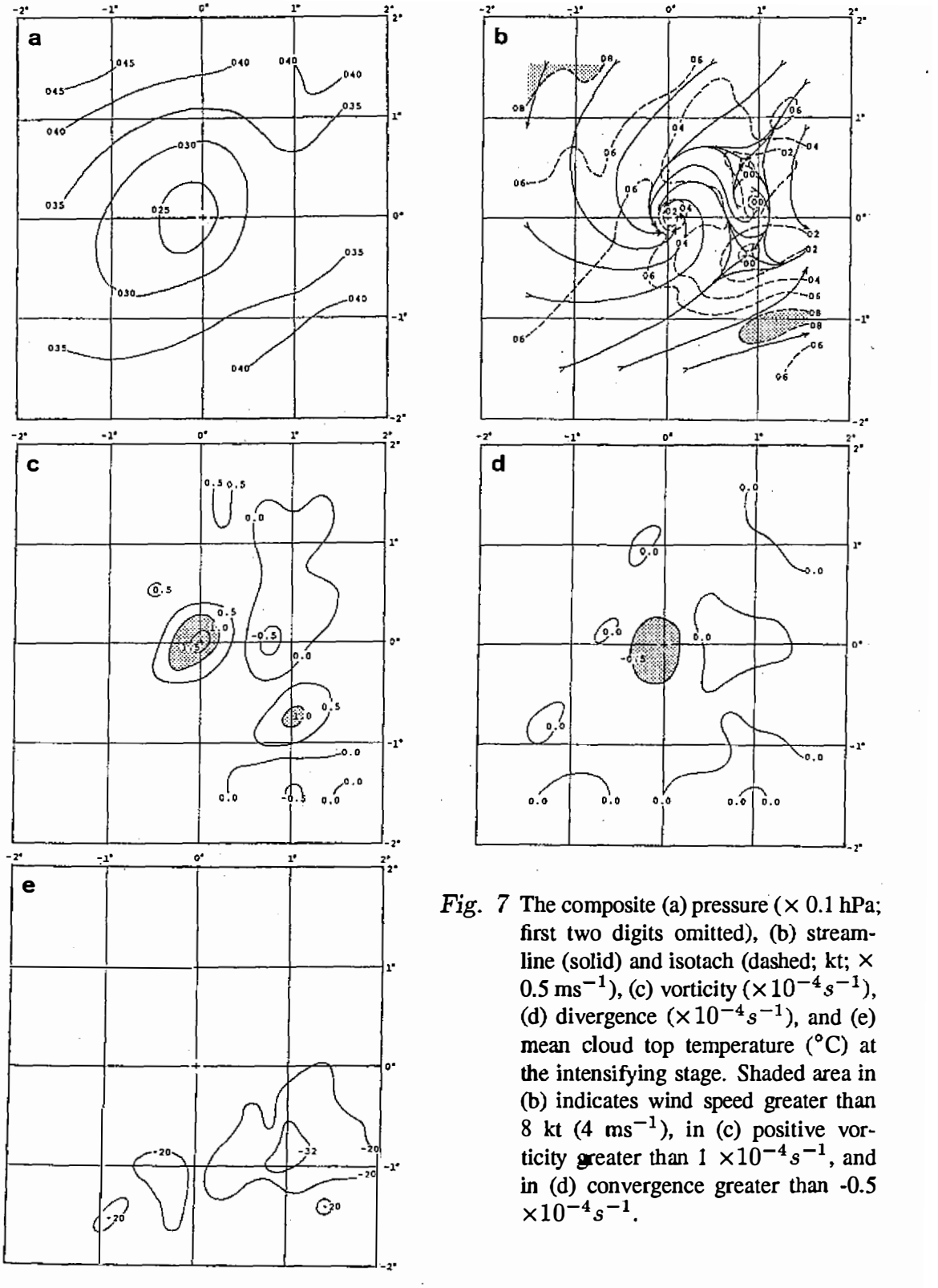


*Fig. 7* The composite (a) pressure (× 0.1 hPa; first two digits omitted), (b) streamline (solid) and isotach (dashed; kt; × 0.5 $ms^{-1}$), (c) vorticity ($\times 10^{-4}s^{-1}$), (d) divergence ($\times 10^{-4}s^{-1}$), and (e) mean cloud top temperature (°C) at the intensifying stage. Shaded area in (b) indicates wind speed greater than 8 kt (4 $ms^{-1}$), in (c) positive vorticity greater than 1 $\times 10^{-4}s^{-1}$, and in (d) convergence greater than -0.5 $\times 10^{-4}s^{-1}$.

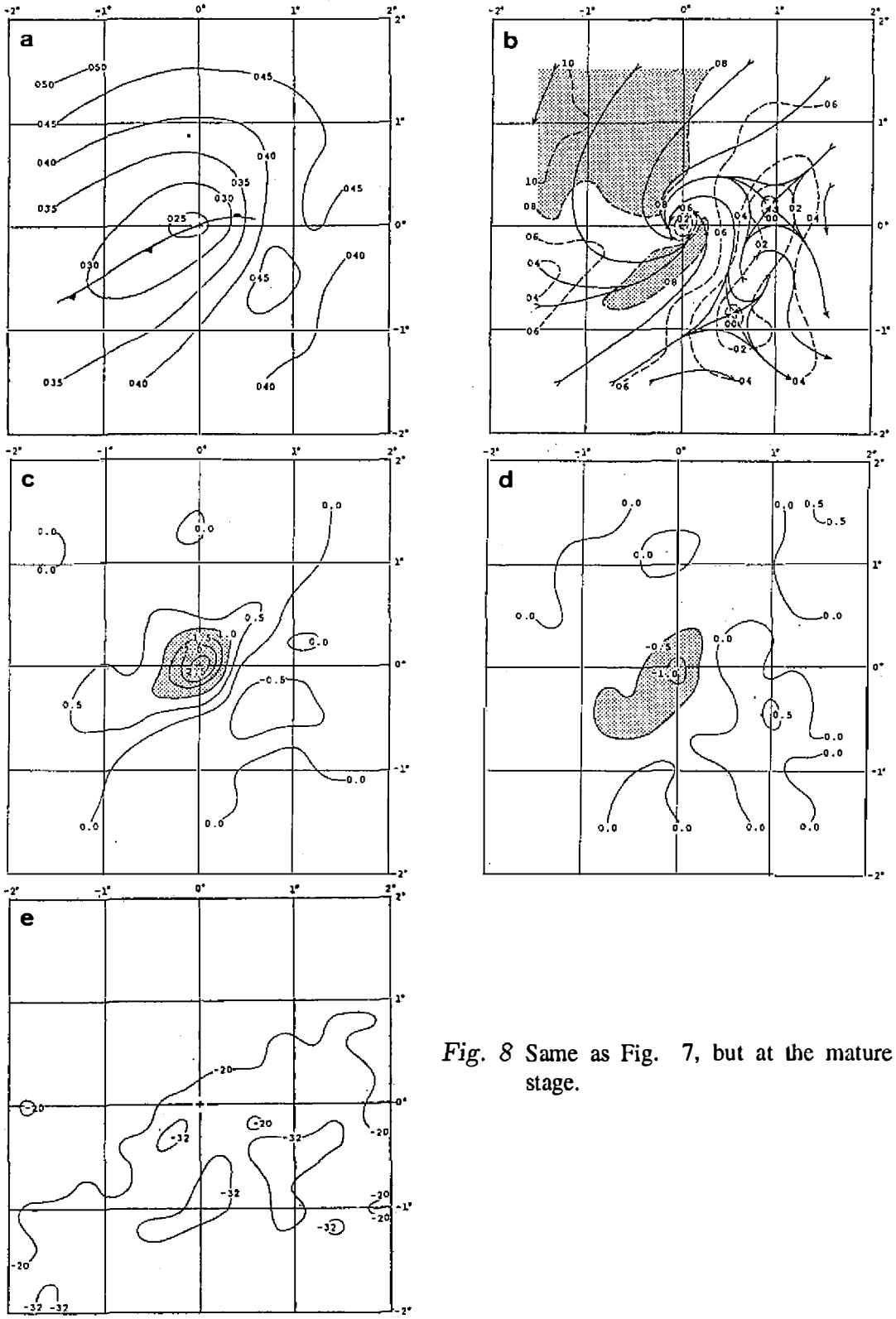


*Fig. 8* Same as Fig. 7, but at the mature stage.

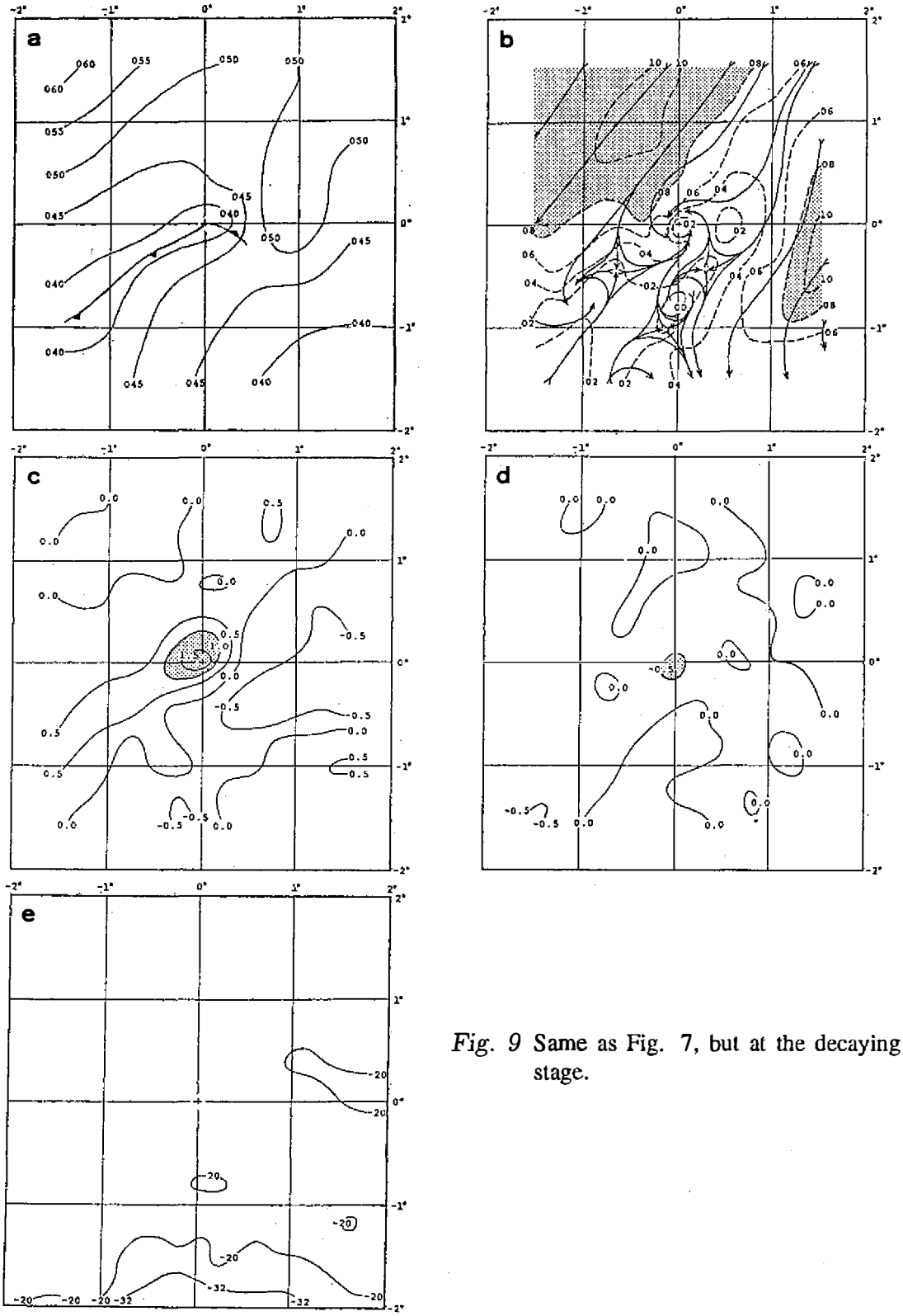


*Fig. 9* Same as Fig. 7, but at the decaying stage.

over the mesolow area, increased from 220 km at the intensifying stage to 270 km at the mature stage, then decreased to 120 km at the decaying stage. Cyclonic vorticity was a maximum over tthe center. It increased from a value of $1.5 \times 10^{-4}$ $s^{-1}$ at the intensifying stage to a value of $2.5 \times 10^{-4}$ $s^{-1}$ at the mature stage, then decreased to a value of $1.5 \times 10^{-4}$ $s^{-1}$ at the decaying stage. Similar changes were observed for the convergence over the low center. Taking $-1.0 \times 10^{-4}$ $s^{-1}$ as an average value of convergence from intensifying to mature stage, it takes less than 2 h to increase the cyclonic vorticity from 1.5 to $2.5 \times 10^{-4}$ $s^{-1}$ solely based on vortex stretching consideration. The average time duration between the intensifying and mature stages, as presented in Table 2, was about 9 h. This again indicated the important role played by the surface boundary layer frictional dissipation process in the mesolow dynamics.

The mean cloud top temperature showed a clear decrease over and to the south of the low center, where the southwesterly wind speed increase was observed, at the mature stage. The frequency of deep convections (not shown) also increased dramatically over the same area. Therefore, the intensity of convective activities, and thus heavy rainfall occurrence, over and to the south of the low center seemed to be closely related to the intensification of the mesolow. This is also supported by the mean cloud top temperature averaged over the cyclonic circulation area of the mesolow at different stages. A value of -3.4°C, -19.3°C, and -8.6°C was obtained at the intensifying, mature, and decaying stages, respectively.

## 5. COMPOSITE STRUCTURE OF DIFFERENT SCALES

Five mesolows, as presented in Tables 1 and 3, can be grossly classified into 2 types. Cases 2 and 5 belong to type A which originated to the west of 118°E and had a larger horizontal scale with heavy rainfall occurrence to the south of the low center. The other 3 cases belong to type B which formed locally to the northwest or southwest of Taiwan and had a small horizontal scale with heavy rainfall occu rence over the mesolow area. Therefore, it seems reasonable to expect the similarities and differences for the different scales of mesolows. Composite structure of meso-$\alpha$ scale (> 200 km) and meso-$\beta$ scale (< 200 km) mesolows was then obtained and presented in Figures 10 and 11. It is clear from Table 3 that the meso-$\alpha$ scale mainly consisted of cases 2 and 5 and the meso-$\beta$ scale consisted of the other 3 cases.

Meso-$\alpha$ scale low had a greater pressure gradient, deeper center pressure, and larger perturbation pressure amplitude as compared to the meso-$\beta$ scale. The wind speed was stronger over the meso-$\alpha$ low area as would be expected from the greater pressure gradient. One of the very interesting features in the wind field was the existence of a southwesterly wind maximum (> 8 kt) to the south of the meso-$\alpha$ low center. This southwesterly wind maximum was also supported by a greater pressure gradient over the same area. The heavy rainfall occurrence to the south of the meso-$\alpha$ scale low center was consistent with the stronger southwesterly flows which presumably had more efficient moisture supply for the deep convections. Meso-$\alpha$ low also had relatively stronger cyclonic vorticity and convergence over the low area. The mean cloud top temperature and frequency of deep convections (not shown) were in agreement with the relative position of heavy rainfall occurrence. The meso-$\alpha$ low had heavy rainfall occurring to the south of the center; the meso-$\beta$ low, over the low area.

## 6. DISCUSSION AND CONCLUSIONS

The mesolows observed to the west of the Central Mountain Range, particularly to the northwest and southwest of Taiwan, have been suggested to be closely related to the heavy

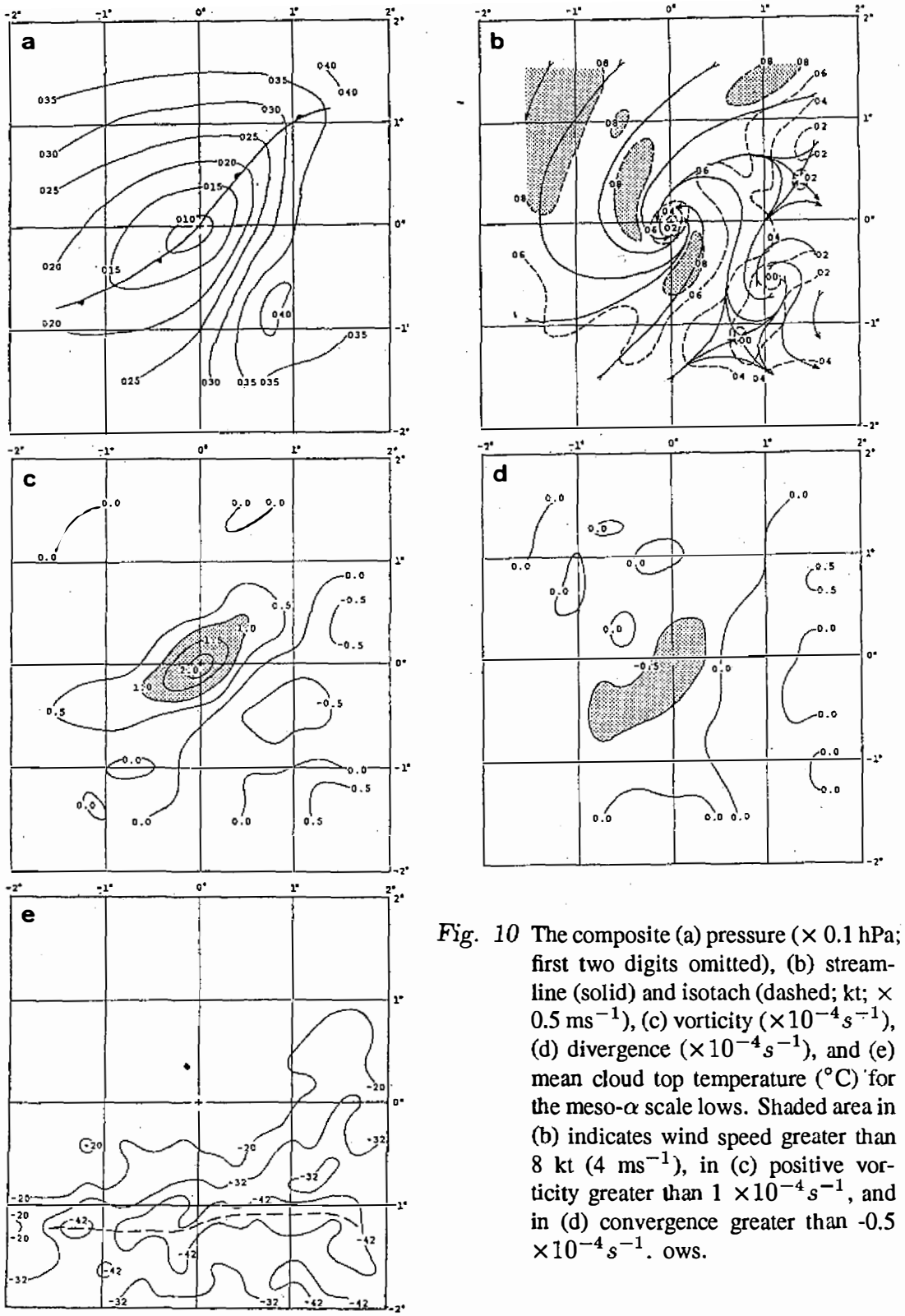


*Fig. 10* The composite (a) pressure (× 0.1 hPa; first two digits omitted), (b) streamline (solid) and isotach (dashed; kt; × 0.5 $ms^{-1}$), (c) vorticity ($\times 10^{-4} s^{-1}$), (d) divergence ($\times 10^{-4} s^{-1}$), and (e) mean cloud top temperature (°C) for the meso-α scale lows. Shaded area in (b) indicates wind speed greater than 8 kt (4 $ms^{-1}$), in (c) positive vorticity greater than 1 $\times 10^{-4} s^{-1}$, and in (d) convergence greater than -0.5 $\times 10^{-4} s^{-1}$. ows.

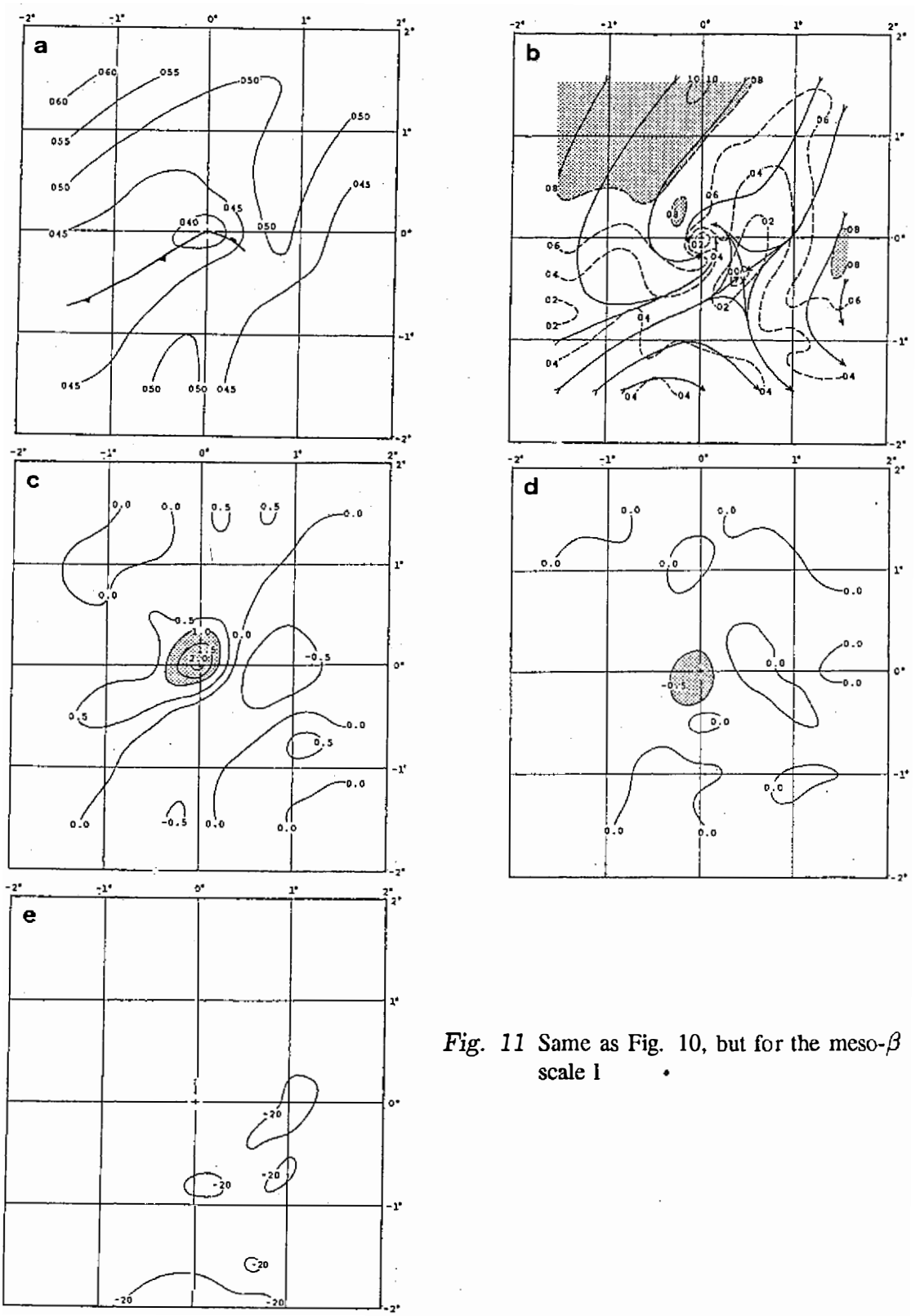


*Fig. 11* Same as Fig. 10, but for the meso-$\beta$ scale I

rainfall event during the Taiwan Mei-Yu season (Chen, 1979; Chen and Chi, 1980; Chen, 1990). However, the basic understanding of questions such as detailed structure and dynamic processes of the mesolow as well as the specific dynamic link between the convection and the mesolow has been greatly hampered by the limited data over the adjacent ocean. To alleviate this problem, the composite technique was employed for 5 cases of mesolows which were accompanied by heavy rainfall over or to the south of the mesolow.

Similarities and differences in structure were found among all of the 5 cases. The mesolow that formed and migrated along the Mei-Yu front (cases 2 and 5) had a larger horizontal scale, a longer time duration, and a deeper center pressure than the other 3 cases. The heavy rainfall for these 2 cases occurred to the south of the mesolow where the convections were also stronger as indicated by the much lower mean cloud top temperature and much higher frequency of deep convections over the same area as compared to the other 3 cases. The mesolow that formed locally to the northwest (case 1) and southwest of Taiwan (cases 3 and 4), on the other hand, had a smaller horizontal scale, a shorter time duration, and a weaker center pressure. The heavy rainfall for these 3 cases occurred over the mesolow area where convections prevailed but were less active than those of the other 2 cases.

For cases 2 and 5, the heavy rainfall occurred to the south of the low center where the stronger southwesterly winds and the greater pressure gradient were observed. This is consistent with what would be expected for the stronger southwesterly flow that presumably had more efficient moisture supply for the deep convections. The fact that heavy rainfall and deep convections occurred, either over the mesolow area or to the south of the low center, over the area of maximum horizontal convergence suggested the important role of the surface boundary layer (frictional) convergence in regulating the behavior of convections. Another possible role played by the surface friction was that it tended to counteract the vortex stretching process in the evolution of the mesocyclone.

The mesolows formed locally over a relatively warm area to the northwest of Taiwan (case 1) and to the southwest of Taiwan (cases 3 and 4) under the prevailing northeasterly flows in agreement with the previous numerical study (Chern and Sun, 1989) and observational studies (Chen *et al.*, 1989; Chen and Hui, 1990; Chen and Liang, 1992). The blocking effect of the CMR of the low-level northeasterly cold air, thus, appeared to be important in the formation of mesolows to the west of the CMR. Although these lows were weaker in the pressure field, they had a similar intensity in cyclonic vorticity and convengence over the low center as compared to the lows migrating along the Mei-Yu front. The stronger winds in the prevailing northeasterly flows, presumably over the ocean area, occurred to the north/northwest of the low center. This suggested that the shear vorticity due to the land-sea differential friction over the mesolow area was perhaps one of the important mechanisms for the formation and maintenance of the mesocyclone to the northwest and southwest of Taiwan.

The composite structure at different life stages showed that a maximum intensity in cyclonic vorticity was reached at mature stage as would be expected from the criteria of stage classification. It is also true for the convergence, the pressure, the mean cloud top temperature, and the frequency of deep convections. An interesting feature at the mature stage was that an area of maximum southwesterly flows developed to the south of the low center where the pressure gradient increased dramatically from the intensifying stage. Therefore, the deep convections and thus the heavy rainfall over and to the south of the mesolow center tended to be closely associated with the formation and intensification of the mesolow through the enhanced southwesterly flows and the boundary layer convergence.

A scale dependence in the structure was observed in the composite of the meso-$\alpha$ and meso-$\beta$ lows. The difference was mainly a reflection of the migrating (meso-$\alpha$ cases

2 and 5) and the locally formed quasi-stationary (meso-$\beta$ cases 1, 3, and 4) lows. The meso-$\alpha$ low had a greater pressure gradient, deeper center pressure, stronger wind, stronger cyclonic vorticity, and greater convergence. The reverse was true for the meso-$\beta$ low. The meso-$\alpha$ low had heavy rainfall and deep convections which occurred to the south of the low center; the meso-$\beta$ low, over the low area. Although cyclonic circulation was observed over the mesolow area for both scales, the cross-isobaric ageostrophic flow was evident. This suggests that a semi-geostrophic model, such as that used by Lin (1989, 1990), is needed in the theoretical and numerical studies of the mesolow.

Using a composite technique, detailed structure was obtained and dynamic processes were inferred for the mesolow to the west of the CMR in the Taiwan Mei-Yu season. The similarities and differences among all of the 5 cases were presented. The time and space-scale dependences of the mesolow were discussed. Results from this study provided observational evidence to the questions of the formation process of the mesocyclone and the dynamic link between the heavy rainfall/deep convections and the mesolow.

**Acknowledgments** Thanks to the Central Weather Bureau for providing the surface and the GMS data. This study was partially supported by the National Science Council under Grant NSC 81-0202-M002-513.

## REFERENCES

Chen, G. T. J., 1978: On the meso-scale systems for the Mei-Yu regime in Taiwan. Proc. Conf. Severe Weather in Taiwan Area, NSC and Academia Sinica. 150-157 (in Chinese with English abstract). [Available from the Dept. of Atmos. Sci., Natl. Taiwan Univ., Taipei, Taiwan, R.O.C.]

Chen, G. T. J., 1979: Mesoscale analysis for a Mei-Yu case over Taiwan. *Papers Meteor. Res.*, **2**, 63-74.

Chen, G. T. J., 1990: Study of rainfalls and radar echoes in the heavy rainfall events accompanied by mesolow in Mei-Yu season. *Atmos. Sci.*, **18**, 213-228 (in Chinese with English abstract).

Chen, G. T. J., 1992: Mesoscale features observed in the Taiwan Mei-Yu season. *J. Meteor. Soc. Japan*, **70**, 367-386.

Chen, G. T. J., and S. S. Chi, 1980: On the mesoscale rainfall and meso-low in the Mei-Yu season in Taiwan. *Atmos. Sci.*, **7**, 39-48 (in Chinese with English abstract).

Chen, G. T. J., and C. C. Yu, 1988: Study of low-level jet and extremely heavy rainfall over northern Taiwan in the Mei-Yu season. *Mon. Wea. Rev.*, **116**, 884-891.

Chen, G. T. J., and C. Y. Liang, 1992: A mid-level vortex observed in the Taiwan Area Mesoscale Experiment (TAMEX). *J. Meteor. Soc. Japan*, **70**, 25-41.

Chen, G. T. J., and C. C. Yu, 1990: Role of Mei-Yu front and mesolow on the heavy rainfall events : Two cases in TAMEX phase I (1986). *Atmos. Sci.*, **18**, 129-147 (in Chinese with English abstract).

Chen, Y. L., and N. B. F. Hui, 1990: Analysis of a shallow front during Taiwan Area Mesoscale Experiment. *Mon. Wea. Rev.*, **118**, 2649-2667.

Chen, Y. L., Y. X. Zhang and N. B. F. Hui, 1989: Analysis of a surface front during the early summer rainy season in Taiwan. *Mon. Wea. Rev.*, **117**, 909-931.

Chern, J. D., and W. Y. Sun, 1989: Lee cyclogenesis and interaction between front and mountain. Proc. Workshop on TAMEX Preliminary Scientific Results, Taipei, 22-30 June, 343- 346. [Available from the Dept. of Atmos. Sci., Natl. Taiwan Univ., Taipei, Taiwan, R.O.C.]

Lin, Y. L., 1989: A study of flow over a mesoscale mountain with diabatic heating. Proc. Workshop on TAMEX Preliminary Scientific Results, Taipei, 22-30 June, 327-333. [Available from the Dept. of Atmos. Sci., Natl. Taiwan Univ., Taipei, Taiwan, R. O. C.]

Lin, Y. L., 1990: A theory of cyclogenesis forced by diabatic heating. Part II: A semi-geostrophic approach. *J. Atmos. Sci.*, **47**, 1755-1777.

# 台灣梅雨季伴隨豪雨之中尺度低壓合成結構

陳泰然
國立台灣大學大氣科學研究所

王重傑
中國文化大學地球科學研究所

## 摘要

本文選取１９８５～８７年台灣梅雨季5個伴隨豪雨之中尺度低壓個案，利用每3小時之地面資料及每3小時之日本同步衛星（GMS）數據化雲頂溫度資料，以合成方法研究個別低壓、不同生命階段之低壓與不同尺度之低壓結構。合成場包括，氣壓、溫度、溫度露點差、流線與等風速線、渦度、散度、平均雲頂溫度及不同雲頂溫度之深對流頻率。

結果顯示，個別中尺度低壓合成結構間存在顯著之相似性與相異性。在梅雨鋒上形成且沿鋒面在台灣海峽東移之低壓，具有較大水平尺度、較長生命期及較深中心氣壓，且豪雨發生在低壓以南之最大輻合區與最強西南氣流區。在台灣西北及西南地區產生之中尺度低壓，豪雨則發生在低壓區域。中央山脈對低層由東北方而來的冷空氣之阻擋效應，顯然爲台灣西北部與西南部中尺度低壓形成之重要因子，而海陸摩擦差異導致之中尺度低壓區內之風切渦度，則爲中尺度氣旋形成與維持之重要機制。

不同生命階段之合成結構顯示發生在低壓中心以南之深對流與豪雨，顯然透過西南氣流和近地層輻合之增強與中尺度低壓之形成和發展密切關連。深對流／豪雨與最大輻合區之密切關係，更顯示邊界層之摩擦輻合效應在決定對流發展之重要角色。此外，結果亦顯示地面摩擦在中尺度氣旋演變過程裡，有抵消渦旋拉伸之旋生效應。最後，不同尺度之結構異同亦存在於中$\alpha$與中$\beta$尺度之低壓，其特徵則類似個別合成低壓之結構。